

## Beyond the Bragg Peak: Hyperthermal Heavy Ion Damage to DNA Components

Zongwu Deng, Ilko Bald,\* Eugen Illenberger,\* and Michael A. Huels†

*Ion Reaction Laboratory, Department of Nuclear Medicine and Radiobiology, Faculty of Medicine and Health Sciences,  
University of Sherbrooke, Sherbrooke, Quebec, J1H 5N4, Canada*

(Received 25 May 2005; published 7 October 2005)

We have observed the destruction of fundamental building blocks of DNA (nucleoside, base, and sugar) by hyperthermal (0.25–1.75 eV/amu) heavy ion impact. Nucleoside damage pathways include base or sugar loss, and complete disintegration of either moiety. Sugar damage dominates, and in DNA will yield a complex strand break. Our results suggest that (a) heavy particle damage to biological media may extend to ion track ends beyond the Bragg peak, and (b) the nascent damage by hyperthermal secondary heavy particles, formed along the primary ion tracks, may be equally complex.

DOI: [10.1103/PhysRevLett.95.153201](https://doi.org/10.1103/PhysRevLett.95.153201)

PACS numbers: 34.50.Dy, 82.30.Fi, 87.14.Gg

Proton, or heavy ion-beam cancer therapy is under rapid development and has achieved significant clinical success [1,2]. It differs from conventional high-energy electron and photon (x- or  $\gamma$ -ray) therapy in that it delivers radiation doses up to an energy-dependent depth, with a maximum dose density deposited at the “Bragg peak” shortly before the track end; conversely, electrons or photons penetrate the irradiated medium with near-exponentially decreasing relative dose density [3,4], and cause high radiation doses to be delivered to healthy tissue upon entrance. An enhancement of relative biological effectiveness (e.g., tumor cell death) is also observed in the Bragg peak [3,4]. These factors result in the two main advantages of tumor treatment with ion beams: volume selectivity and high efficiency for deep-seated tumors [5]. It is presently believed that heavy ion irradiation causes DNA damage via similar pathways as conventional ionizing radiation [6,7], involving mainly simple ionization, single bond cleavage, and slow radical attack, but modulated by the different structure and higher ionization density of the ion track.

However, in addition to its unique dose distribution, another significant difference between ion and conventional radiotherapy should be noted: recent measurements by Schlathöler *et al.* [8,9] have shown that along the radiation track of a primary heavy particle (MeV range), significant amounts of secondary atomic cations with hyperthermal energies up to several hundreds of eV can be produced from DNA bases. Because the secondary ion energy is much higher than that produced by conventional ionizing radiation using electrons and photons, this suggests that (a) the initial DNA damage created during ion therapy will be different, and (b) the nascent DNA damage by the secondary fragments will also involve more complex mechanisms than simple ionization, and slow radical reactions. In dense media, energetic secondary ions produced along the primary ion track will scatter inelastically over short distances (several nm), and may induce complex DNA damage clusters that cannot be repaired by the cell.

For similar reasons, DNA damage at the primary ion track ends, i.e., at macroscopic distances beyond the Bragg peak, is also of consequence, since it often involves dam-

age to regions beyond the tumor volume, which likely contain important healthy organs. Since at track ends the remaining primary ion energy (several 100 eV) is also deposited on nanometer scales, similar DNA damage clusters as those induced by the secondary ions may result. While the possibility of such potentially lethal DNA lesions is of great biological importance, the propensity of either low energy secondary ions, or primary ion track ends, to cause such damage is as of yet unknown, and is thus neglected from radiation track calculations, or risk estimates.

Here we report measurements of ion induced fragmentation of fundamental DNA components in the condensed phase at precisely such low ion energies in the 10–100 eV range. The DNA components studied are thymidine (dT, a fundamental base-sugar complex nucleoside), the DNA base thymine (T), and 2-deoxy-D-ribose (dR, the fundamental sugar subunit of the sugar-phosphate backbone in DNA). Our experiments reveal several specific, previously unknown, pathways of ion induced DNA damage that may occur during heavy particle irradiation of cells, and that reach far beyond simple ionization, or single bond cleavage.

The experiments were carried out on an ultra-high-vacuum (UHV) ion-beam system at the Sherbrooke laboratory, to be described in detail elsewhere. Briefly, the system delivers a well focused, mass- and energy-resolved, positive ion beam in the 1–500 eV energy range into a UHV reaction chamber for sample irradiation. The measured energy spread of the cation beams used here is  $\sim 1$  eV full width at half maximum over the entire ion energy range. Beams of 20–30 nA  $\text{Ar}^+$  ions, focused at the target to a 2–4 mm spot, are used in the present experiments. In the reaction chamber a quadrupole mass spectrometer (QMS) is installed perpendicularly to the ion-beam axis to monitor desorbing positive and negative ions during primary ion impact. The QMS measures desorbed ions with *in vacuo* energies between 0 and 5 eV. During experiments, the sample surface is oriented at  $30^\circ$  with respect to the incident ion-beam axis, and at  $60^\circ$  relative to the QMS. Multilayer films of DNA components are pre-

pared by *in vacuo* evaporation onto an electrically isolated, atomically clean polycrystalline Pt substrate, held on a manipulator at room temperature (16–22 °C). Film deposition rates are monitored *in situ* in a load-lock chamber by a quartz crystal microbalance, and are calibrated to within 5 ng/cm<sup>2</sup>. Here we use films of 200 ng/cm<sup>2</sup>, which corresponds to about 4–5 nominal monolayers (MLs) for either compounds, which are evaporated at 130–140 °C (dT), 90–110 °C (T) and 45–50 °C (dR). All compounds (Sigma Aldrich) are 99.5% pure, verified for dT by high-pressure liquid chromatography. dT and T are also purified in the load lock by degassing at 35–40 °C. The Pt substrate is cleaned by flash heating to 1000 °C, followed by 200 eV Ar<sup>+</sup> SIMS, prior to each film deposition.

Figure 1 shows the ion stimulated desorption (ISD) mass spectra along with the chemical composition of positive and negative ions desorbing from films of (a) thymine (T), (b) 2-deoxy-D-ribose (dR) and (c) thymidine (dT) during 100 eV (2.5 eV/amu) Ar<sup>+</sup> ion irradiation. The chemical identification of the fragments of thymine is achieved by measuring and comparing mass spectra of thymine and thymine-methyl-d<sub>3</sub>-6-d [10]. Notably, the most abundant cation fragment at 28 amu is assigned uniquely to an HNCH<sup>+</sup> ion, originating exclusively from bond cleavage at the N1-C6 site of thymine, rather than a CO<sup>+</sup> ion. The fragments of 2-deoxy-D-ribose are identified in the present experiments by measuring and comparing ISD mass spectra of 2-deoxy-D-ribose, D-ribose, and isotope-labeled D-ribose (5-<sup>13</sup>C and 1D D-ribose, Cambridge isotopes, 99% isotopic purity).

The identification of thymidine fragments is therefore accomplished by comparison with those of thymine and 2-deoxy-D-ribose. Overall, the cation mass spectrum below 80 amu is similar to that of 2-deoxy-D-ribose, except for the increase in relative intensity of the 28, 54, and 55 amu peaks which are attributed to the HNCH<sup>+</sup>, HNC<sub>3</sub>H<sub>3</sub><sup>+</sup> (or NC<sub>3</sub>H<sub>4</sub><sup>+</sup>), and HNC<sub>3</sub>H<sub>4</sub><sup>+</sup> fragments of thymine. It thus

appears that in the basic nucleoside thymidine, most of the low mass cation fragments *originate from the sugar moiety*. Note particularly the formation of H<sub>3</sub>O<sup>+</sup> ions. Above 80 amu, the two fragments at 127 amu and 110 amu are assigned to [T + H]<sup>+</sup> and [T-O]<sup>+</sup>, respectively. The fragment at 117 amu is the whole sugar moiety of thymidine and is labeled here as [dR-OH]<sup>+</sup>. Note that the fragments [T + H]<sup>+</sup> and [dR-OH]<sup>+</sup> are indicative of release of the whole base or sugar moiety. The negative ion fragments of thymidine can be attributed mainly to the fragmentation of either the base (CN<sup>-</sup>, OCN<sup>-</sup>), or the sugar moiety (OH<sup>-</sup>, hydrocarbon anions) or both (H<sup>-</sup>, O<sup>-</sup>).

Figure 2 shows the relative desorption yields of the major cation fragments from thymidine films as a function of incident Ar<sup>+</sup> energy, from which the fragment desorption energy thresholds are derived. The desorption energy thresholds of the major positive and negative ion fragments are summarized in Table I. Fragment desorption occurs at energy thresholds down to about 10 eV (0.25 eV/amu) with anion fragments desorbing at higher energies than cation fragments. The detailed ISD dynamics is discussed elsewhere in the case of thymine [11]. In ISD experiments on dielectric solids, fragment ions must possess sufficient kinetic energy to overcome the about 1–1.5 eV charge induced polarization barrier at the surface of the film [12]. As a consequence, molecular damage in the film is likely to continue at energies somewhat below the present desorption thresholds, yielding, however, ionic fragments with kinetic energies insufficient for desorption from the film.

In the following, we highlight the radiobiological relevance of several specific fragments induced here by hyperthermal ion impact to thymidine. [T + H]<sup>+</sup> and [dR-OH]<sup>+</sup> fragments are indicative of glycosidic bond cleavage of thymidine, as is the [T-O]<sup>+</sup> fragment, which is also associated with C = O bond scission. The release of thymine and other nonmodified bases via glycosidic bond cleavage

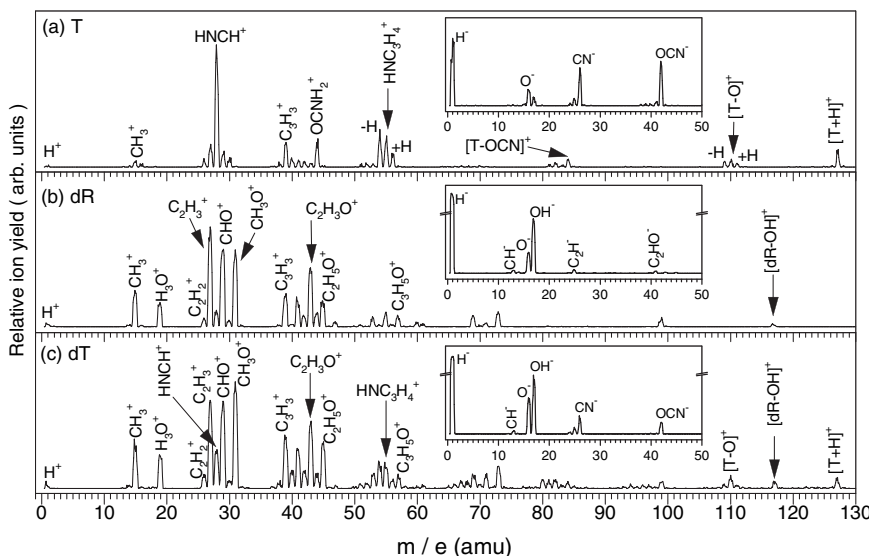


FIG. 1. Cation and anion (insets) desorption mass spectra produced by 100 eV Ar<sup>+</sup> impact on films of (a) thymine (T), (b) 2-deoxy-D-ribose (dR), and (c) thymidine (dT); each film is about 4 nominal monolayers (4 ML ≈ 200 ng/cm<sup>2</sup>) on a Pt substrate.

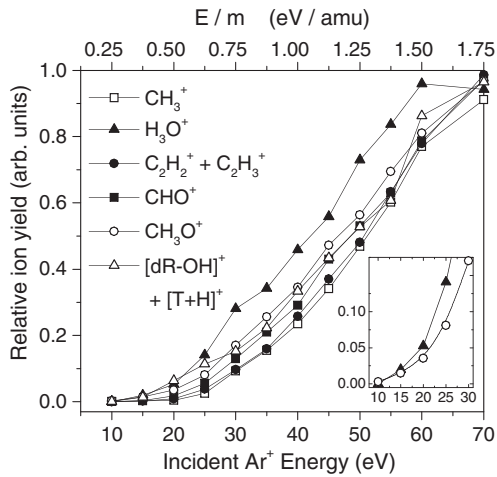


FIG. 2. Desorption energy thresholds for cation fragments produced by  $\text{Ar}^+$  impact on thymidine films (4 ML). The relative ion yields are normalized in intensity at 70 eV. The inset shows a close-up for  $\text{H}_3\text{O}^+$  and  $\text{CH}_3\text{O}^+$ .

is an important pathway of DNA damage (base loss) as a consequence of exposure to conventional ionizing radiation [13,14]. This damage has been attributed to the chemical oxidation of DNA [15–17] and low energy secondary electron attachment [18]. The present results suggest that primary or secondary ions with energy down to 15 eV can also cause damage to DNA via glycosidic bond cleavage. It proceeds most likely via a close interaction between an incident cation and the carbon or nitrogen atom of the glycosidic bond, which ionizes and excites the molecule via localized charge exchange and ultimately breaks the chemical bond. In this respect, the  $[\text{dR-OH}]^+$  fragment can be a result of direct glycosidic bond cleavage, whereas the formation of  $[\text{T} + \text{H}]^+$  fragments from thymidine requires the abstraction of *two* hydrogen atoms by the initial  $[\text{T} - \text{H}]^+$  from its surrounding medium.

The formation of  $\text{H}_3\text{O}^+$  ions is another clear evidence of H abstraction from thymidine (and 2-deoxy-D-ribose) by hydroxyl cations originating from the sugar moiety. H loss is also an important pathway of DNA damage during exposure to conventional ionizing radiation [13,19,20]. For example, a radiolytic H radical can abstract H atoms

to form unscavengable  $\text{H}_2$  products [13], and secondary electron attachment can selectively eliminate N-bound hydrogen from the bases [19,20]. H abstraction by radiolytic OH radicals was also observed with low rate constants [13]. Here, however, primary ion impact leads to formation of  $\text{OH}^+$  (from the sugar moiety in thymidine) which abstracts two other hydrogen atoms from its parent or adjacent thymidine [21]. The formation of  $\text{H}_2\text{DO}^+$  ions during  $\text{Ar}^+$  ion irradiation of 1D D-ribose suggests abstraction of H specifically from the C1 atom site. The abundant  $\text{H}_3\text{O}^+$  ion yield also suggests a high efficiency of H abstraction. This may result from the high mobility of the  $\text{OH}^+$  fragment obtained from the ion impact, as well as its high reactivity. H abstraction by ionic fragments is probably driven by their affinity for hydrogen to yield thermodynamically more stable final products. In the case of  $[\text{T} + \text{H}]^+$  formation, it is demonstrated by the formation of abundant  $\text{T}^+$  ions during 70 eV electron impact of gas phase thymine (no access to hydrogen) [10] and its complete conversion into  $[\text{T} + \text{H}]^+$  ions during ion impact on condensed phase thymine [Fig. 1(a)] [10,11].

Furthermore, ion impact also results in severe fragmentation of both the sugar moiety and the base at energies down to 10 eV. This is quite different from the effects of conventional radiation (x or  $\gamma$  rays) which mainly involve simple ionization or single bond cleavage. Here, the  $\text{HNCH}^+$  and  $\text{HNC}_3\text{H}_4^+$  fragments involve the N1 atom of thymine and are indicative of base loss via complete base fragmentation. However, fragmentation of the sugar moiety is more severe than that of the base. Use of isotope-labeled D-ribose reveals that all the chemical bonds of the sugar moiety are fragile under 10–30 eV  $\text{Ar}^+$  ion impact. In addition,  $\sim 52\%$  of the  $\text{C}_2\text{H}_3^+$ ,  $\sim 18\%$  of the  $\text{CHO}^+$ , and  $\sim 33\%$  of the  $\text{CH}_3\text{O}^+$  sugar fragments involve the C5 position of the sugar (as observed here by use of 5- $^{13}\text{C}$  substituted D-ribose), which in DNA will constitute a *complex* strand break *involving multiple bond rupture*, as opposed to “frank” strand breaks involving single bond cleavage. While the latter may be easily repaired in DNA, the former are likely not. Given the abundant fragment species originating from the sugar moiety shown in Fig. 1, their high desorption yields and low desorption energy thresholds, fragmentation of the sugar appears to be an important pathway of heavy ion damage to thymidine. In other words, in ion irradiated DNA the sugar backbone is likely to be more fragile than the nucleic acid base.

Recent studies on high-energy ion interactions with gas phase biomolecules have shown that secondary ions (singly or multiply charged) with energies up to several hundred electron volts will be produced along radiation tracks [8,9]. In the present study, the abundant and efficient fragmentation pathways of DNA components by ion impact at comparable (or lower) secondary ion energies suggest that even the secondary ions can induce further damage to DNA, which is supported by the observation of single and double strand breaks in double stranded DNA

TABLE I. Desorption energy thresholds (DETs) in eV (eV/amu) for the major ion fragments produced by  $\text{Ar}^+$  ion impact on thymidine films. The experimental uncertainty in the threshold values is  $\pm 2$  eV, except for those marked with asterisk ( $+ 5 / - 2$  eV).

| DET in eV<br>(eV/amu) | Fragments  |
|-----------------------|--|
| 10 (0.25)             | $\text{H}_3\text{O}^+$ , $\text{CH}_3\text{O}^+$ , $\text{C}_2\text{H}_5\text{O}^+$ , $\text{C}_2\text{H}_3\text{O}^+$ |
| 15 (0.38)             | $\text{CHO}^+$ , $\text{C}_2\text{HO}^+$ , $[\text{dR-OH}]^{+*}$ , $[\text{T-O}]^{+*}$ , $[\text{T} + \text{H}]^{+*}$  |
| 20 (0.5)              | $\text{CH}_3^+$ , $\text{C}_2\text{H}_3^+$ , $\text{C}_3\text{H}_3^+$ , $\text{HNCH}^+$ , $\text{H}^-$ , $\text{OH}^-$ |
| 35 (0.88)             | $\text{O}^-$ , $\text{CN}^-$ , $\text{OCN}^-$  |

induced by 100 eV Ar<sup>+</sup> ion impact [22]. This damage will be highly clustered, involve multiple bond breaks, and will be hard to repair. The primary ions can continue to induce complex localized damage clusters at the final track ends, even at energies near 0.25 eV/amu (here, 10 eV for Ar<sup>+</sup>). Hence, DNA damage at the Bragg peak itself, and more importantly at track ends beyond the Bragg peak, is likely more complex than traditionally assumed. In combination with the unique dose distribution of heavy particle irradiation, which suggests the production of abundant secondary ions in the Bragg peak, the primary as well as secondary ion induced damage may thus account for the enhancement of relative biological effectiveness of heavy ion radiation.

While present global models of cellular radiolysis do not include effects of hyperthermal secondary ions, or individual primary ion track ends, our results show that they may be significant, and should be accounted for in dose models or radiation risk estimates. Heavy particle beams contain a statistical distribution of many individual ion Bragg peaks with certain range straggling of (usually several mm [23]) superimposed in the tumor volume, while the distance from the beam's Bragg peak maximum to its track (beam) end can be several tens of mm [4]. Thus, at the very track ends of individual ions, or in the low dose region beyond the beam's Bragg peak, significant damage to DNA may also occur, and may lead to subtle and unexpected changes to the genome.

In summary, we have studied the fragmentation of important DNA building blocks (thymidine, thymine, and 2-deoxy-D-ribose) induced by hyperthermal heavy ion irradiation. Use of isotope-labeled molecules reveals the site specificity of the dominant fragments. Heavy ion impact on thymidine, even below 1 eV/amu, leads to the release of the whole base, the sugar moiety, and the desorption of abundant low mass ring fragments from both. However, the sugar moiety in thymidine is significantly more sensitive to hyperthermal ion attack than the base. Some of the reactive fragments can abstract hydrogens from adjacent thymidine to desorb as protonated fragments. Our results suggest several specific pathways of DNA damage by primary ion impact, including complex strand breaks at the sugar backbone, that may occur during heavy particle radiotherapy of tumors, particularly given the abundant energetic secondary ions produced therein. Our results suggest that nascent DNA damage mechanisms by ion tracks reach far beyond conventional models of simple ionization, single bond cleavage, or slow radical damage. This challenges the traditional views that (a) DNA damage by heavy ion tracks involves similar nascent transients and damage pathways as those initiated by conventional ( $\gamma$ - or x-ray) radiation tracks, and (b) that the higher relative biological effectiveness of ion tracks is determined mainly by the different structure and higher ionization density of the ion track compared to conventional radiation tracks.

This work is continuously supported by NSERC. A CIHR grant funded construction of the ion-beam system,

and a NATO grant allowed staff travel to Sherbrooke (I.B.).

---

\*Permanent address: Institut für Chemie—Physikalische und Theoretische Chemie, Freie Universität Berlin, Takustrasse 3, D-14195 Berlin, Germany.

†Corresponding author.

michael.huels@usherbrooke.ca

- [1] M. Goitein, A. J. Lomax, and E. S. Pedroni, *Phys. Today* **55** No. 9, 45 (2002).
- [2] D. Schulz-Ertner, A. Nikoghosyan, C. Thilmann, T. Haberer, O. Jäkel, C. Karger, G. Kraft, M. Wannenmacher, and J. Debus, *Int. J. Radiat. Oncol. Biol. Phys.* **58**, 631 (2004).
- [3] M. Scholz, *Nucl. Instrum. Methods Phys. Res., Sect. B* **161–163**, 76 (2000).
- [4] H. Stelzer, *Nucl. Phys. B, Proc. Suppl.* **61**, 650 (1998).
- [5] U. Weber, W. Becher, and G. Kraft, *Phys. Med. Biol.* **45**, 3627 (2000).
- [6] S. Brons, G. Taucher-Scholz, M. Scholz, and G. Kraft, *Radiat. Environ. Biophys.* **42**, 63 (2003).
- [7] M. Krämer and G. Kraft, *Adv. Space Res.* **14**, 151 (1994).
- [8] J. de Vries, R. Hoekstra, R. Morgenstern, and T. Schlathöler, *Phys. Rev. Lett.* **91**, 053401 (2003).
- [9] T. Schlathöler, R. Hoekstra, and R. Morgenstern, *Int. J. Mass Spectrom.* **233**, 173 (2004).
- [10] M. Imhoff, Z.-W. Deng, and M. A. Huels, *Int. J. Mass Spectrom.* **245**, 68 (2005).
- [11] Z.-W. Deng, M. Imhoff, and M. A. Huels, *J. Chem. Phys.* (to be published); I. Bald, Z.-W. Deng, E. Illenberger, and M. A. Huels (to be published).
- [12] M. A. Huels, L. Parenteau, M. Michaud, and L. Sanche, *Phys. Rev. A* **51**, 337 (1995).
- [13] C. von Sonntag, *The Chemical Basis for Radiation Biology* (Taylor and Francis, London, 1987).
- [14] S. G. Swarts, M. D. Sevilla, D. Becker, C. J. Tokar, and K. T. Wheeler, *Radiat. Res.* **129**, 333 (1992).
- [15] J. R. Wagner, C. Decarroz, M. Berger, and J. Cadet, *J. Am. Chem. Soc.* **121**, 4101 (1999).
- [16] Y. Razskazovskiy, M. G. Debije, and W. A. Bernhard, *Radiat. Res.* **153**, 436 (2000).
- [17] E. S. Henle, R. Roots, W. R. Holley, and A. Chatterjee, *Radiat. Res.* **143**, 144 (1995).
- [18] Y. Zheng, P. Cloutier, D. J. Hunting, J. R. Wagner, and L. Sanche, *J. Am. Chem. Soc.* **126**, 1002 (2004).
- [19] H. Abdoul-Carime, S. Gohlke, and E. Illenberger, *Phys. Rev. Lett.* **92**, 168103 (2004).
- [20] M.-A. Hervé du Penhoat, M. A. Huels, P. Cloutier, J.-P. Jay-Gerin, and L. Sanche, *J. Chem. Phys.* **114**, 5755 (2001).
- [21] This observation will be discussed in a forthcoming publication (Ref. [11]).
- [22] L. Sellami, F. Martin, D. Hunting, S. Lacombe, and M. A. Huels, in *Proceedings of the Yearly Meeting of the American Physical Society, Montreal, Canada, 2004, Abstracts of Contributed Papers* (American Physical Society, College Park, Maryland, 2004).
- [23] M. Hollmark, J. Uhrdin, Dž Belkić, I. Gudowska, and A. Brahme, *Phys. Med. Biol.* **49**, 3247 (2004).